The Astrophysical Journal Letters, 776:L14 (6pp), 2013 October 10 doi:10.1088/2041-8205/776/1/L14

DETECTION OF PROPENE IN TITAN'S STRATOSPHERE

C. A. Nixon[1], D. E. Jennings[2], B. Bézard[3], S. Vinatier[3], N. A. Teanby[4], K. Sung[5], T. M. Ansty[6], P. G. J. Irwin[7], N. Gorius[8], V. Cottini[9], A. Coustenis[3], and F. M. Flasar[1]
[1] Planetary Systems Laboratory, NASA Goddard Space Flight Center, Greenbelt, MD 20771, USA
[2] Detector Systems Branch, NASA Goddard Space Flight Center, Greenbelt, MD 20771, USA
[3] LESIA, Observatoire de Paris, CNRS, 5 Place Jules Janssen, F-92195 Meudon Cedex, France
[4] School of Earth Sciences, University of Bristol, Wills Memorial Building, Queen's Road, Bristol BS8 1RJ, UK
[5] Jet Propulsion Laboratory, California Institute of Technology, 4800 Oak Grove Drive, CA 91109, USA
[6] Department of Space Science, Cornell University, Ithaca, NY 14853, USA
[7] Atmospheric, Oceanic and Planetary Physics, University of Oxford, Clarendon Laboratory, Parks Road, Oxford OX1 3PU, UK
[8] IACS, Catholic University of America, Washington, DC 20064, USA
[9] Department of Astronomy, University of Maryland, College Park, MD 20742, USA
Received 2013 June 28; accepted 2013 September 11; published 2013 September 30

ABSTRACT

The *Voyager 1* flyby of Titan in 1980 gave a first glimpse of the chemical complexity of Titan's atmosphere, detecting many new molecules with the infrared interferometer spectrometer (IRIS). These included propane (C_3H_8) and propyne (CH_3C_2H), while the intermediate-sized C_3H_x hydrocarbon (C_3H_6) was curiously absent. Using spectra from the Composite Infrared Spectrometer on *Cassini*, we show the first positive detection of propene (C_3H_6) in Titan's stratosphere (5σ significance), finally filling the three-decade gap in the chemical sequence. We retrieve a vertical abundance profile from 100–250 km, that varies slowly with altitude from 2.0 ± 0.8 ppbv at 125 km, to 4.6 ± 1.5 ppbv at 200 km. The abundance of C_3H_6 is less than both C_3H_8 and CH_3C_2H, and we remark on an emerging paradigm in Titan's hydrocarbon abundances whereby *alkanes* > *alkynes* > *alkenes* within the C_2H_x and C_3H_x chemical families in the lower stratosphere. More generally, there appears to be much greater ubiquity and relative abundance of triple-bonded species than double-bonded, likely due to the greater resistance of triple bonds to photolysis and chemical attack.

Key words: planets and satellites: atmospheres – planets and satellites: composition – planets and satellites: individual (Titan)

1. INTRODUCTION

Titan, largest satellite of Saturn, is unique amongst moons by virtue of its deep atmosphere, consisting mostly of nitrogen and methane (∼95% and ∼5%, respectively, in the troposphere; Niemann et al. 2005). These two molecules are disintegrated, mainly by solar UV photons and Saturn magnetospheric electrons in the upper atmosphere, with fragments recombining to give rise to a plethora of organic molecules. These include hydrocarbons (C_xH_y) and nitriles ($C_xH_y[CN]_z$), many of which were first identified in Titan's stratosphere by the infrared interferometer spectrometer (IRIS) on *Voyager 1* during the 1980 flyby (Hanel et al. 1981; Kunde et al. 1981; Maguire et al. 1981). Prior to the arrival of *Cassini* in 2004, further molecules, including the oxygen-bearing species CO, CO_2, and H_2O (Lutz et al. 1983; Samuelson et al. 1983; Coustenis et al. 1998), and later CH_3CN and C_6H_6 (Marten et al. 2002; Coustenis et al. 2003) were spectroscopically detected in Titan's atmosphere using a variety of ground- and space-based observatories. More recently the *Cassini* Ion and Neutral Mass Spectrometer has discovered an even greater diversity (Vuitton et al. 2007; Cui et al. 2009) in the upper atmosphere (ionosphere).

Regarding the stratospheric hydrocarbons, the C_2H_x series of acetylene (or ethyne, C_2H_2), ethylene (or ethene, C_2H_4), and ethane (C_2H_6) were all firmly detected by IRIS, confirming earlier ground-based observations. Of the C_3H_x species, methylacetylene (or propyne, CH_3C_2H) and propane (C_3H_8) were first identified by Maguire et al. (1981) from IRIS data. Others in the sequence including allene (CH_2CCH_2), isomer of propyne; and the alkene molecule propene (or propylene, C_3H_6); and its isomer cyclopropane (see Figure 1), have not been identified spectroscopically during the 32 yr since *Voyager*.

In this Letter we report the first detection of propene in Titan's stratosphere using spectra from the *Cassini* Composite Infrared Spectrometer (CIRS), filling an important gap in the C_3H_x family, and providing insights into the relative abundances of alkanes, alkenes, and alkynes in Titan's atmosphere. In Section 2 we discuss our observations and data analysis method; in Section 3 we present our results; in Section 4 we discuss the context and implications of this discovery; and Section 5 is our conclusions.

2. METHODS

2.1. Data Set

The spectra analyzed in this work were recorded by CIRS (Flasar et al. 2005) during flybys of Titan at ranges 100,000–200,000 km (∼5–10 hr from closest approach), and at the highest resolution of CIRS, 0.5 cm^{-1}, apodized, with the focal plane three (FP3; 600–1100 cm^{-1}) and four (FP4; 1100–1400 cm^{-1}) detector arrays. These are parallel arrays of 10 pixels each, with square fields of view 0.273 mrad across, giving projected footprints of 27–54 km for this data set. At these ranges, CIRS performs limb-viewing observations (MIRLMBINT), placing the linear arrays perpendicular to the disk edge, and viewing ten altitudes at a single latitude. The arrays are then repositioned upward, acquiring spectra at 10 further altitudes.

Limb views are ideal both for measuring vertical profiles of important constituents, but also for detections of the least abundant species, since limb rays traverse a longer optical path through the atmosphere than rays from the surface. Therefore, we co-added large numbers of limb spectra to search for previously undetected molecular signatures. We binned spectra from FP3 and FP4 separately, at 25 km altitude increments

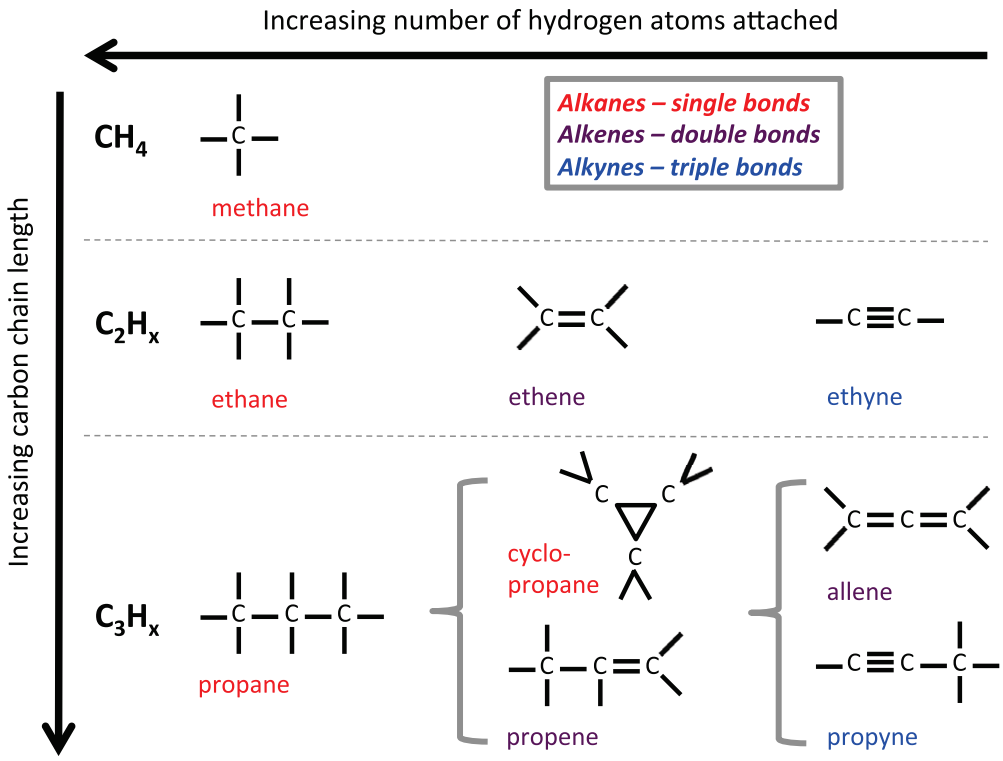

Figure 1. Small hydrocarbon molecules. Note that the two isomers of C_3H_6 (cyclopropane and propene), along with CH_2CCH_2 (allene), have not previously been detected in Titan's stratosphere.

Table 1
Retrieved Abundances for C_3H_x and C_2H_x Hydrocarbons at Five Altitudes

Alt. (km)	Press. (mbar)	N_{spec}	$q(C_2H_2)$ (ppmv)[a]	$q(C_2H_4)$ (ppmv)[a]	$q(C_2H_6)$ (ppmv)[a]	$q(C_3H_4)$ (ppbv)[b]	$q(C_3H_6)$ (ppbv)[b]	$q(C_3H_8)$ (ppbv)[b]
125	4.64	356	1.83 ± 0.10	0.23 ± 0.05	6.2 ± 1.2	7.8 ± 1.6	2.0 ± 0.8	621 ± 133
150	2.41	443	2.15 ± 0.09	0.16 ± 0.03	7.6 ± 1.3	9.7 ± 1.8	2.6 ± 0.8	619 ± 122
175	1.31	561	2.71 ± 0.11	0.11 ± 0.02	9.5 ± 1.6	11.0 ± 1.9	4.6 ± 1.2	846 ± 158
200	0.74	570	2.96 ± 0.13	0.06 ± 0.01	12.3 ± 2.0	9.4 ± 1.7	4.6 ± 1.5	872 ± 171
225	0.42	570	2.88 ± 0.13	0.04 ± 0.01	8.9 ± 1.9	9.5 ± 2.1	2.6 ± 1.6	757 ± 171

Notes.
[a] ppmv = parts per million by volume.
[b] ppbv = parts per billion by volume.

with 50 km bin width, ensuring Nyquist sampling of vertical information. After consideration of the available observations, we restricted the latitudes to 30°S–10°N, at times from 2004 July 1 to 2010 July 1. These ranges were selected as a compromise between homogeneity within the sample (low latitudes show the least seasonal variation; Teanby et al. 2010; Bampasidis et al. 2012), while allowing for a large enough set to have high signal-to-noise ratio (S/N). The numbers of spectra in each altitude bin—centered on five altitudes 125, 150, 175, 200, 225 km—are given in Table 1.

2.2. Radiative Modeling and Inversion

The modeling proceeded in two steps: first, the FP4 spectra were analyzed to obtain ambient temperature information at each altitude, by modeling the methane ν_4 band at 1305 cm^{-1}. The methane vertical profile was taken from measurements by the *Huygens* GCMS (Niemann et al. 2010; 0–140 km), and assumed constant at $1.48\% \pm 0.09\%$ above 140 km throughout the stratosphere and mesosphere as expected from photochemical models (Wilson & Atreya 2004). Then, the temperature profile was fixed, and the FP3 spectral region was modeled to obtain abundances of multiple hydrocarbon species (C_2H_2, C_2H_4, C_2H_6, CH_3C_2H, and C_3H_8) previously identified in Titan's stratosphere.

The spectral modeling and fitting used the NEMESIS computer code (Irwin et al. 2008), that has previously been widely utilized to model outer planet infrared spectra, including Titan (e.g., de Kok et al. 2007a, 2007b; Teanby et al. 2007, 2009; Nixon et al. 2009a, 2009b, 2010, 2012; Cottini et al. 2012). Details can be found in these publications; only a brief overview of the modeling is given here, emphasizing changes to previous work. The spectral lines for each gas were derived mainly from the HITRAN (CH_4; Rothman et al. 2009) and GEISA atlases (C_2H_2, C_2H_4, C_2H_6; Jacquinet-Husson et al. 2011). The exceptions were CH_3C_2H, which used an unpublished line list maintained at Paris Observatory (see Vinatier et al. 2007, for description), and propane, which used a new pseudo-line list model compiled at the Jet Propulsion Laboratory (JPL; Sung et al. 2013). This new list enabled us to fit for the first time several propane bands not included in

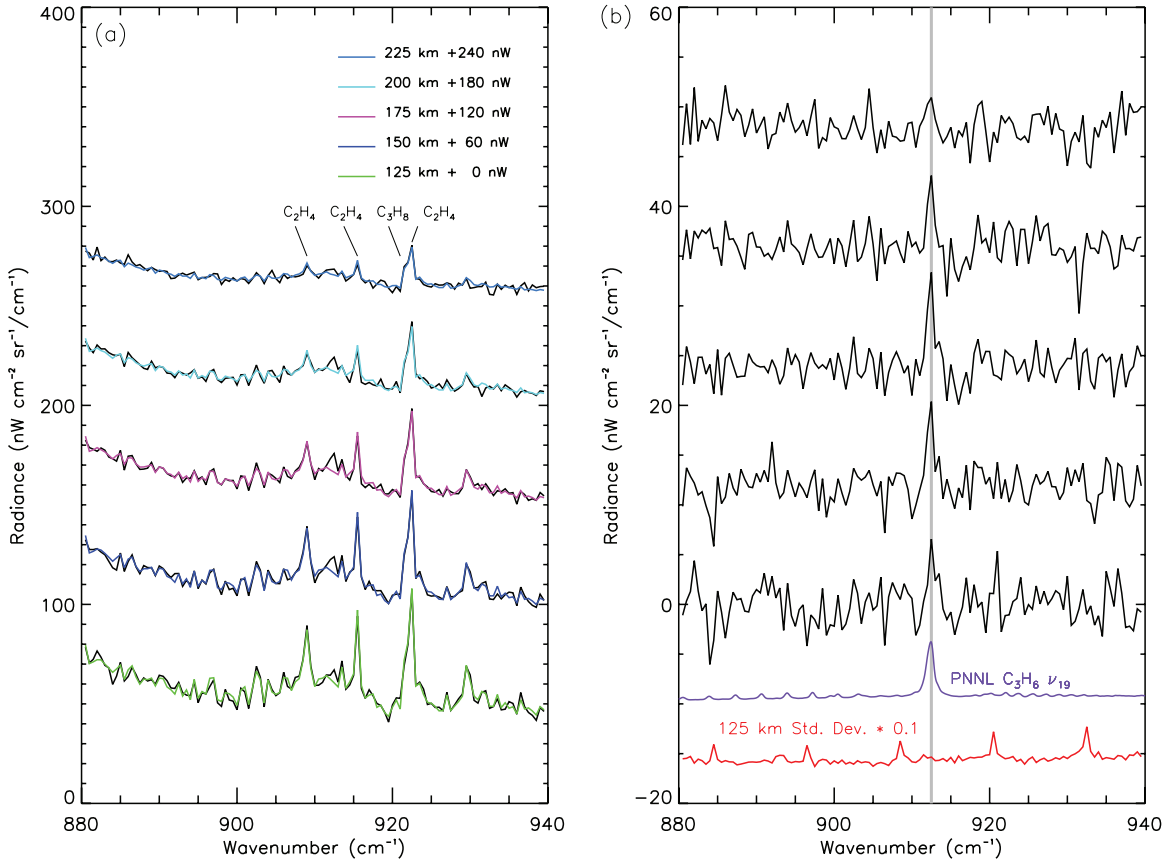

Figure 2. (a) Five spectral averages of Titan limb data (black) and the best-fit model spectra (colors), as described in the text. Data/model spectral pairs at each altitude have been vertically offset in radiance for clarity (see legend). (b) The "residual" emission not modeled (black), formed by subtracting data–model spectra. Residuals at each altitude are sequentially offset by 12 nW from the next lower altitude. The purple line is the 278 K laboratory absorbance spectrum of propene for comparison (not in radiance units), showing the location of the ν_{19} band at 912.5 cm^{-1}. The red line shows the standard deviation of the spectral average at 125 km (others are similar), scaled by $\times 0.1$ and -20 nW offset, showing that the locations of noise artifacts (vertical "spikes") are not coincident with the propene ν_{19} emission.

pre-existing line compilations, in the spectral region from 800 to 1300 cm^{-1}.

The inversion algorithm minimizes a "cost function," similar to a χ^2 goodness-of-fit parameter, as explained in Irwin et al. (2008). Vertical profiles for the five known C_2H_x and C_3H_x hydrocarbon gases and a gray aerosol haze were thus retrieved, since there is continuous vertical information in the five overlapping vertical bins. On FP3 we retrieved abundances from the following spectral sub-ranges: 600–650 cm^{-1} for CH_3C_2H, 700–760 cm^{-1} for C_2H_2, 800–900 cm^{-1} for C_2H_6, and 850–950 cm^{-1} for C_2H_4 and C_3H_8; fitting the haze opacity independently for each range, in addition to further gases having overlapping bands (HCN, C_4H_2, C_6H_6, HC_3N, CO_2) that are not discussed in this Letter. These ranges also required us to fit three separate bands of propane: the ν_{26} at 748 cm^{-1}, the ν_8 at 869 cm^{-1}, and the ν_{21} at 922 cm^{-1}, which was critical for the eventual detection of propene at 912 cm^{-1}, described in Section 3. The continuum across the 850–950 cm^{-1} spectral range could not be well fitted using a gray haze opacity, or other standard haze opacity (Khare et al. 1984). Therefore, we derived our own continuum haze opacity, by applying a 30 point (= 15 cm^{-1}) boxcar smoothing kernel to the residual, and re-fitting the gases using this smoothed baseline for the haze opacity.

3. RESULTS

Figure 2(a) shows the spectral averages for FP3 in the range 880–940 cm^{-1} (in black), along with the final model fits (colored lines). This spectral region is characterized by lines of the ethylene ν_7 band at 909, 915.5, 922.5 cm^{-1} and from the ν_{21} band of propane with a Q-branch at 922 cm^{-1}, modeled here using the new JPL pseudo-linelist. Note the "missing" emission in the model spectrum at 912.5 cm^{-1}, more easily seen on Figure 2(b), which shows the residual after the model is subtracted from the data. This 912.5 cm^{-1} emission occurs in the precise location of the ν_{19} band of propene (C_3H_6) (Lafferty et al. 2006). For comparison, at the bottom of Figure 2(b) we show a laboratory (5°C) absorbance ($-\log_{10}(I/I_0)$) spectrum of propene recorded at the Pacific Northwest National Laboratory (PNNL; Sharpe et al. 2004) confirming the feature location. The PNNL spectrum was smoothed from a native resolution of 0.112 cm^{-1} (boxcar apodization) to the CIRS resolution of 0.5 cm^{-1} (Hamming apodized), and has a peak absorbance at 912.5 cm^{-1} (in arbitrary units). To rule out any possible instrumental artifacts, we also show (in red) above each residual spectrum the corresponding standard deviation of the individual spectra in the average. Some small peaks occur due to electrical interference in the CIRS instrument, but none of these falls at 912.5 cm^{-1}.

To increase S/N and improve the detection of propene, we averaged the non-overlapping 125, 175, and 225 km averages, ensuring no duplicate information, each weighted by the N_{spec} of Table 1. This average, along with the weighted best-fit spectrum, is shown in Figure 3(a). We also show the model calculation with the new (JPL pseudo-linelist) lines of propane not included, i.e., a spectrum due to ethylene and the continuum only. The residuals from both models (propane and non-propane) are

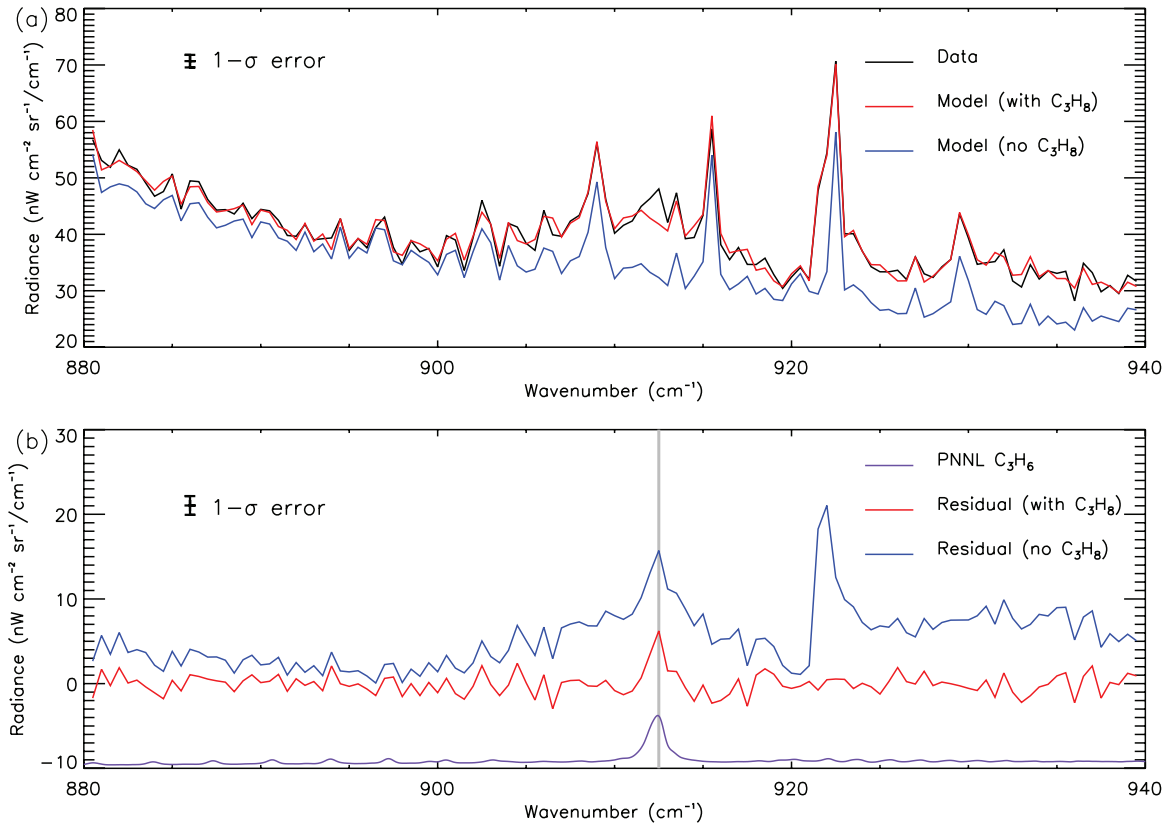

Figure 3. (a) Co-added data spectrum (black) from weighted average of lowest (125 km), middle (175 km), and topmost (225 km) vertical bins. Weights are N_{spec} from Table 1. Also shown are the model spectra with propane (red) and without propane (blue) from the JPL pseudo-line list. (b) Residuals from subtracting data–model: blue line is model without propane and red line is with propane. The purple line shows the smoothed laboratory absorbance spectrum of propene recorded at PNNL, scaled by 1×10^4 and offset by -10. The detection significance is $\sim 5\sigma$.

shown in the lower panel (b), illustrating that the propene emission at 912.5 cm^{-1} is not part of the propane P-band emission (the broad bump from ~905–920 cm^{-1}).

A spectral line listing for propene is not yet available, so we cannot include C_3H_6 in our radiative transfer model to retrieve its abundance. However we can estimate its abundance from that of propane, by comparing the relative strengths of their emissions. The radiance (I) of optically thin spectral lines is proportional to both the gas abundance (q) and the spectral absorption cross-section (k). If we additionally assume that the emission in limb viewing originates mostly from the tangent altitude z, where the atmospheric pressure is p, temperature is T_z, and Planck function is $B(\tilde{\nu}, T_z)$, then we can write

$$I(\tilde{\nu}, z) \propto k(\tilde{\nu}) f(\tilde{\nu}, T_z, T_0) q(z) p(z) B(\tilde{\nu}, T_z), \quad (1)$$

where $f(\tilde{\nu}, T_z, T_0)$ is a first-order correction factor to the overall band strength for the temperature-dependence of the occupancy of the energy states using Boltzmann statistics, similar to Equation (A11) of Rothman et al. (1998):

$$f(\tilde{\nu}, T_z, T_0) = \frac{\exp(-c_2\tilde{\nu}/T_z)/V(T_z)}{\exp(-c_2\tilde{\nu}/T_0)/V(T_0)}. \quad (2)$$

In the above formula, T_0 is the temperature of the laboratory measurements (278 K), c_2 is the second radiation constant $hc/k = 1.4388$ cm K, and $V(T)$ is the total vibrational partition function defined in Equation (B.6) of Nixon et al. (2009a). By writing this radiance formula separately for the propane emission at 922 cm^{-1} and propene at 912.5 cm^{-1}, then taking ratios, and canceling the Planck functions and ambient pressures, we find

$$q_{C_3H_6}(z) = q_{C_3H_8}(z) \left(\frac{k(922.0)}{k(912.5)}\right) \times \left(\frac{f(922.0, T_z, 278)}{f(912.5, T_z, 278)}\right) \left(\frac{I(912.5, z)}{I(922.0, z)}\right). \quad (3)$$

The emission (I) at 912.5 and at 922.0 cm^{-1} is obtained from the residual of spectral fitting (i.e., from the blue and red curves of Figure 3(b)), while the absorption cross-sections (cm^2 molecule^{-1}) were obtained from the 278 K absorbance spectra of C_3H_8 and C_3H_6 using the conversion factor of 9.28697×10^{-16} recommended by PNNL. The absorption cross-sections were smoothed to the requisite resolution and extracted at 912.5 and 922.0 cm^{-1}. Some assumptions in this technique may give rise to systematic errors, in particular the simple scaling we have used for band intensities from laboratory (278 K) to Titan stratospheric temperatures. Although this may account reasonably well for the principal "cold bands" of each gas (transitions from ground state), the contribution of hot bands to the observed emission features is unknown and is therefore the major source of uncertainty.

Figure 4 shows the final results. Panel (a) shows the temperature retrieval from the methane ν_4 band, along with the averaging ranges, while panels (b) and (c) show the gas abundances for the C_2H_x and C_3H_x hydrocarbons respectively, all derived from modeling the individual gas bands except in the case of propene. Note that for the propane vertical profile we used the retrieved abundances from the ν_{21} band, although the ν_8 and ν_{26}

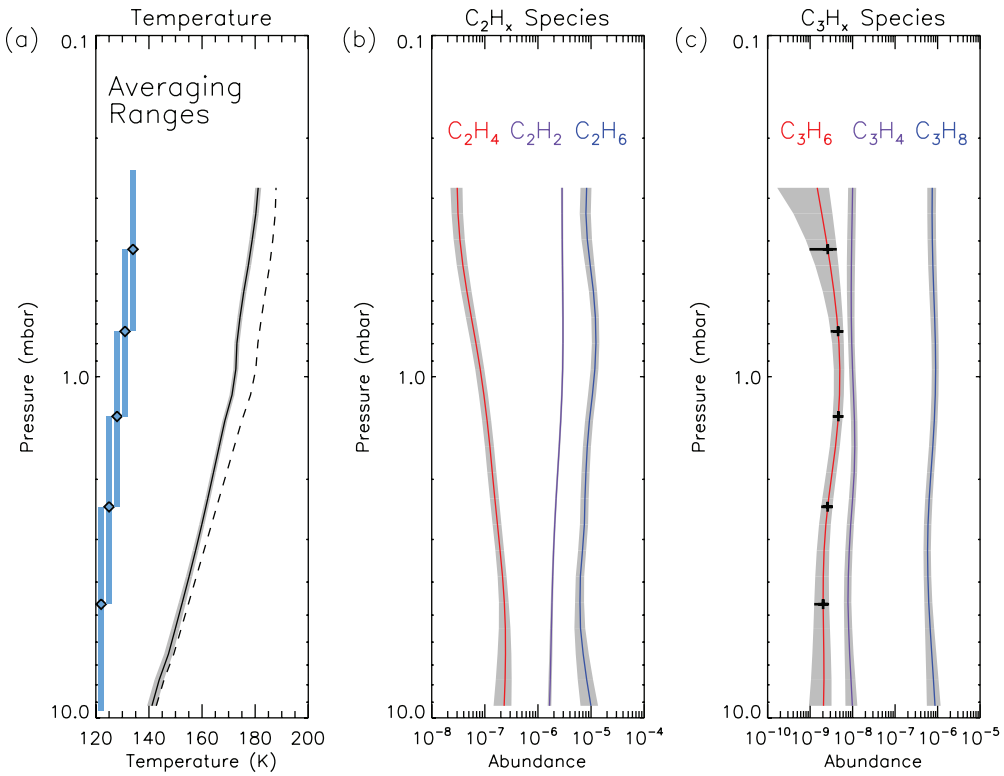

Figure 4. (a) A priori (dashed line) and retrieved temperature profile (solid line) from 100 to 250 km and error estimate (gray). Vertical blue bars show the overlapping averaging ranges for each spectral average, centered on 125, 150, 175, 200, 225 km with 50 km width. (b) Retrieved vertical profiles for the C_2H_x hydrocarbons. (c) Retrieved vertical profiles for the C_3H_x hydrocarbons. The propene abundance is estimated from the emission as described in the text.

bands were also fitted. A detailed intercomparison of propane retrievals from the various bands using the JPL pseudo-linelist will be the subject of a forthcoming paper.

In the case of propene, the emission ratioing technique (Equation (3)) was used to derive its abundance at the five altitudes, and subsequently interpolated using cubic splines onto the same, closer-spaced altitude grid range (100–250 km) as the other gases. The propene error bars were estimated by adding in quadrature the radiance relative error of the propene emission, the abundance relative error of the propane, from which the propene is scaled, and systematic uncertainties in the laboratory cross-section determination of both gases:

$$\Delta q_{C_3H_6} = q_{C_3H_6} \times \left\{ \left(\frac{\Delta q_{C_3H_8}}{q_{C_3H_8}} \right)^2 + \left(\frac{\Delta I_{912.5}}{I_{912.5}} \right)^2 + 2\sigma_{cs}^2 \right\}^{1/2}. \quad (4)$$

The value of σ_{cs} for both C_3H_8 and C_3H_6 is estimated by PNNL at 3% total from all sources, including gas purity, pressure and temperature stability in the cell, etc. Table 1 gives the abundances at each of the five altitudes. Our derived gas profiles for the five previously known species are in good qualitative and quantitative agreement with those of Vinatier et al. (2010) at 20°S (see their Figure 3), although showing somewhat less vertical structure, likely due to the long time-base of these averages. The abundance of propene in the stratosphere is estimated here for the first time, ranging from 2.0 ± 0.8 ppbv at 100 km, to a maximum of 4.6 ± 1.5 ppbv at 200 km, and possibly declining above.

4. DISCUSSION

Propene has previously been detected by submillimeter techniques in a dark interstellar (molecular) cloud, TMC-1 by Marcelino et al. (2007), the first and to our knowledge the only prior astronomical sighting of this molecule. The species C_3H_6 has also been inferred from *Cassini* mass spectrometry of Titan's upper atmosphere as the cause of the signal at 42 amu, with an abundance of 2.3–3.4 ppmv at 1050 km (Magee et al. 2009). However, mass spectra alone cannot distinguish between isomers, so an uncertainty remained as to whether the species was propene or cyclopropane. Therefore, our result constitutes the first definitive detection of propene in a non-terrestrial planetary atmosphere.

C_3H_6 is an important component of photochemical models of Titan's atmosphere and has been included in reaction schemes for C_3H_x since the earliest post-*Voyager* models (Yung et al. 1984). *Cassini*-era models have also necessarily included C_3H_6 (e.g., Wilson & Atreya 2004; Lavvas et al. 2008a, 2008b; Wilson & Atreya 2009; Krasnopolsky 2009, 2010; Vuitton et al. 2012), but few have published stratospheric abundance predictions for propene, apparently due to the lack of observational detection. A vertical profile for propene is given in Wilson & Atreya (2004), showing an abundance of a few ppbv between 100 and 200 km, and positive vertical gradient, in approximate agreement with our results. Propene is also shown in the three versions of the Krasnopolsky model (Krasnopolsky 2009, 2010, hereafter K09 and K10). However, the gas profiles in the K09 and K10 models (defined by escape, and no escape of CH_4, respectively) are much too steep, not just for propene, but for all the hydrocarbon species. The third variant of the model, in Appendix A of K09, which uses a different eddy diffusion profile (recommended by Hörst et al. 2008), predicts a propene abundance of $2–7 \times 10^{-8}$ at 100–200 km, significantly in excess of our findings. In all three versions, the abundance of C_3H_6 is comparable, or greater than that of CH_3C_2H below 500 km, in contradiction with our results.

Recently, Hébrard et al. (2013) has critically re-examined and updated the photochemistry of all C_3H_x species. In their reaction scheme, at 1000 km propene is principally produced by the reactions: $H+C_3H_5 \rightarrow C_3H_6 + h\nu$ (62%) and $CH+C_2H_6 \rightarrow C_3H_6 + H$ (37%). However, in the stratosphere, propene may be produced by other mechanisms, including the termolecular reaction: $CH_3 + C_2H_3 + M \rightarrow C_3H_6 + M$. Important loss mechanisms at these altitudes are (1) photodissociation, and (2) $H + C_3H_6 + M \rightarrow C_3H_7 + M$. The predicted stratospheric abundances of Hébrard et al. (2013) range from $\sim 10^{-10}$ at 100 km to $\sim 7 \times 10^{-10}$ at 200 km, somewhat less than our findings, and also with a significantly steeper gradient. However, Hébrard et al. (2013) caution that their results are not expected to be fully valid below 200 km due to chemical processes not included in the model, such as the effects of cosmic rays.

We remark on an emerging trend amongst the abundances of small hydrocarbons in Titan's lower atmosphere, summarized as *alkanes* (C–C single bonds) > *alkynes* (C≡C triple bonds) > *alkenes* (C=C double bonds). This is now evident for both the C_2H_x family ($C_2H_6 > C_2H_2 > C_2H_4$) and the C_3H_x family ($C_3H_8 > CH_3C_2H > C_3H_6$). Therefore, the ordering of abundances does not follow the sequence of molecular size, or bond saturation, with alkynes being more plentiful than alkenes. A possible explanation is that alkynes, once the strong triple bond has formed, are relatively more secure than alkenes, with the weaker double bond.

Indeed, the phenomenon of more abundant triple-bonded molecules than double-bonded ones extends beyond the hydrocarbons in Titan's stratosphere, and is reflected in the roster of detected species. Nitrogen has *only* been found in Titan's lower atmosphere thus far in triple-bonded form (either N≡N or C≡N). In all, nine molecules with triple bonds have been detected: N_2, CO, C_2H_2, CH_3C_2H, HCN, CH_3CN, HC_3N, C_4H_2, C_2N_2: the latter three with two triple bonds apiece. In contrast, only three double-bonded species are found: CO_2, C_2H_4, and now C_3H_6. Therefore, triple bonds, once formed, appear to be persistent in Titan's atmosphere.

5. CONCLUSIONS

In this Letter we have demonstrated the first definitive detection of propene (C_3H_6) in an extra-terrestrial planetary atmosphere, with an inferred abundance of ~2–5 ppbv (Table 1). This fills a long-standing gap in the C_3H_x series of known aliphatic hydrocarbons in Titan's stratosphere and will provide important additional constraint on photochemical models. We have also demonstrated an apparent trend in hydrocarbon abundances for the lower atmosphere: *alkanes* > *alkynes* > *alkenes*, within each of the C_2H_x and C_3H_x chemical families, and speculate that the triple bond is more resistant to photolysis or chemical attack than the double bond. This picture is undoubtedly simplistic and detailed photochemical modeling is required to elucidate the details, including the role played by cyclic molecules.

Our thanks to Linda Brown (JPL) and Steven Sharpe (PNNL) for providing us with molecular spectroscopic data for propane and propene: absorbances and line lists. C.A.N., D.E.J., N.G., T.M.A., and F.M.F. were supported by the NASA *Cassini* Mission. Part of the research was carried out at the Jet Propulsion Laboratory, California Institute of Technology, under a contract with the National Aeronautics and Space Administration. V.C. was supported by the NASA Post-Doctoral Program. N.A.T. and P.G.J.I. received support for their portion of this work from the UK STFC, and NAT received additional support from the Leverhulme Trust. B.B., S.V., and A.C. were supported by the Centre National d'Études Spatiales (CNES).

Facility: Cassini

REFERENCES

Bampasidis, G., Coustenis, A., Achterberg, R. K., et al. 2012, ApJ, 760, 144
Cottini, V., Nixon, C. A., Jennings, D. E., et al. 2012, Icar, 220, 855
Coustenis, A., Salama, A., Lellouch, E., et al. 1998, A&A, 336, L85
Coustenis, A., Salama, A., Schulz, B., et al. 2003, Icar, 161, 383
Cui, J., Yelle, R. V., Vuitton, V., et al. 2009, Icar, 200, 581
de Kok, R., Irwin, P. G. J., Teanby, N. A., et al. 2007a, Icar, 191, 223
de Kok, R., Irwin, P. G. J., Teanby, N. A., et al. 2007b, Icar, 186, 354
Flasar, F. M., Achterberg, R. K., Conrath, B. J., et al. 2005, Sci, 308, 975
Hanel, R., Conrath, B., Flasar, F. M., et al. 1981, Sci, 212, 192
Hébrard, E., Dobrijevic, M., Loison, J. C., et al. 2013, A&A, 552, A132
Hörst, S. M., Vuitton, V., & Yelle, R. V. 2008, JGRE, 113, E10006
Irwin, P. G. J., Teanby, N. A., de Kok, R., et al. 2008, JQSRT, 109, 1136
Jacquinet-Husson, N., Crepeau, L., Armante, R., et al. 2011, JQRST, 112, 2395
Khare, B. N., Sagan, C., Arakawa, E. T., et al. 1984, Icar, 60, 127
Krasnopolsky, V. A. 2009, Icar, 201, 226
Krasnopolsky, V. A. 2010, P&SS, 58, 1507
Kunde, V. G., Aikin, A. C., Hanel, R. A., et al. 1981, Natur, 292, 686
Lafferty, W. J., Flaud, J.-M., & Herman, M. 2006, JMoSt, 780, 65
Lavvas, P., Coustenis, A., & Vardavas, I. 2008a, P&SS, 56, 27
Lavvas, P. P., Coustenis, A., & Vardavas, I. M. 2008b, P&SS, 56, 67
Lutz, B. L., de Bergh, C., & Owen, T. 1983, Sci, 220, 1374
Magee, B. A., Waite, J. H., Mandt, K. E., et al. 2009, P&SS, 57, 1895
Maguire, W. C., Hanel, R. A., Jennings, D. E., Kunde, V. G., & Samuelson, R. E. 1981, Natur, 292, 683
Marcelino, N., Cernicharo, J., Agúndez, M., et al. 2007, ApJL, 665, L127
Marten, A., Hidayat, T., Biraud, Y., & Moreno, R. 2002, Icar, 158, 532
Niemann, H. B., Atreya, S. K., Bauer, S. J., et al. 2005, Natur, 438, 779
Niemann, H. B., Atreya, S. K., Demick, J. E., et al. 2010, JGRE, 115, 12006
Nixon, C. A., Achterberg, R. K., Teanby, N. A., et al. 2010, FaDi, 147, 65
Nixon, C. A., Jennings, D. E., Flaud, J.-M., et al. 2009a, P&SS, 57, 1573
Nixon, C. A., Teanby, N. A., Calcutt, S. B., et al. 2009b, ApOpt, 48, 1912
Nixon, C. A., Temelso, B., Vinatier, S., et al. 2012, ApJ, 749, 159
Rothman, L. S., Gordon, I. E., Barbe, A., et al. 2009, JQSRT, 110, 533
Rothman, L. S., Rinsland, C. P., Goldman, A., et al. 1998, JQSRT, 60, 665
Samuelson, R. E., Maguire, W. C., Hanel, R. A., et al. 1983, JGR, 88, 8709
Sharpe, S. W., Johnson, T. J., Sams, R. L., et al. 2004, ApSpe, 58, 1452
Sung, K., Toon, G. C., Mantz, A. W., & Smith, M. A. H. 2013, Icar, 226, 1499
Teanby, N. A., Irwin, P. G. J., de Kok, R., & Nixon, C. A. 2010, ApJL, 724, L84
Teanby, N. A., Irwin, P. G. J., de Kok, R., et al. 2007, Icar, 186, 364
Teanby, N. A., Irwin, P. G. J., de Kok, R., et al. 2009, Icar, 202, 620
Vinatier, S., Bézard, B., Fouchet, T., et al. 2007, Icar, 188, 120
Vinatier, S., Bézard, B., Nixon, C. A., et al. 2010, Icar, 205, 559
Vuitton, V., Yelle, R. V., Lavvas, P., & Klippenstein, S. J. 2012, ApJ, 744, 11
Vuitton, V., Yelle, R. V., & McEwan, M. J. 2007, Icar, 191, 722
Wilson, E. H., & Atreya, S. K. 2004, JGRE, 109, 6002
Wilson, E. H., & Atreya, S. K. 2009, JPCA, 113, 11221
Yung, Y. L., Allen, M., & Pinto, J. P. 1984, ApJS, 55, 465